CROATICA CHEMICA ACTA CCACAA 63 (1) 99—112 (1990)

CCA-1924

YU ISSN 0011-1643
UDC 543
Original Scientific Paper

The Effect of the Carrier Gas Flow Rate and Observation Height on Analyte Emission in an Argon ICP

Nada Kovačić, Bojan Budič, Elizabeta Kozak, and Vida Hudnik

Boris Kidrič Institute of Chemistry P. O. Box 30, 61115 Ljubljana, Yugoslavia

Received July 26, 1989

This paper reports on the influence of the carrier gas flow rate and observation height on electron number density, excitation temperature, and the departure from LTE in an argon ICP. Axial analyte distribution for several atomic and ionic lines was measured.

INTRODUCTION

The carrier gas flow rate and observation height are among the most significant parameters in an argon ICP. An increase of the carrier gas flow rate provides a higher sample amount in the plasma, but the residence time of analyte atoms and ions in the plasma becomes shorter causing changes in analytical signal[1-11]. In addition to the residence time, the observation height defines whether atom- or ion-emission prevails in the plasma. The physical parameters of an argon ICP, such as the electron number density and excitation temperature, are mostly determined by the carrier gas flow rate and observation height. Electron number density is an important parameter which governs the excitation processes in the plasma. The excitation of the analyte occurs in the injection channel of an argon ICP which is a relatively cool region. It was established that there is no complete LTE (Local thermodynamic equilibrium) in the injection channel of an argon ICP, usually used in spectrochemical practice as excitation source[9,23-26]. The extent of LTE departure is determined partly by the carrier gas flow rate and observation height which are thus important parameters to be studied and optimized.

The purpose of the current paper is to investigate the effect of the carrier gas flow rate and observation height on the temperature and the electron number density, as well as on the analyte emission in the channel of an argon ICP. In order to determine the consequences of the changes in physical parameters, analytical performances for several ion and atom lines were evaluated in terms of the signal-to-background ratio. The extent of departure from LTE in the channel of argon ICP was discussed.

EXPERIMENTAL

An ARL-3520 OES sequential vacuum spectrometer equipped with SAS 11 computer system for instrument control and data acquisition was used. Instrumental and operating conditions are listed in Table I.

TABLE I

Instrumental and operating conditions

Spectrometer	Monochromator with 1m-radius concave grating in Paschen-Runge mounting
Grating	1080 grooves/mm with reciprocal linear dispersion 0.026 nm/mm; resolution: 1 st order 0.054 nm
Slit widths	Primary: 20 μm Secondary: 50 μm
RF Generator	Quartz-controlled, 27.12 MHz and automatching network operating power 1.2 kW
Plasma torch	Fassel type; inner diameter of injection tube 1 mm
Nebulizer	Glass, concentric Meinhard type
Argon flow rate	Carrier 0.6—1.5 l/min Plasma 0.8 l/min Coolant 12 l/min
Observation height	10—18 mm above the load coil

The uncertainty of the measured intensity was 3‰.

Reagents

High purity acids were used for the preparation of all solutions. The investigated elements were present at the concentration of 10 μg ml^{-1}. The concentration of Fe in the solution used for temperature measurements was 500 $\mu g/ml^{-1}$.

Determination of Excitation Temperature

Excitation temperature in the channel of an argon ICP was determined by applying two different methods (the slope method and the absolute single radiance method) and two different species (Ar and Fe spectral lines). The slopes were

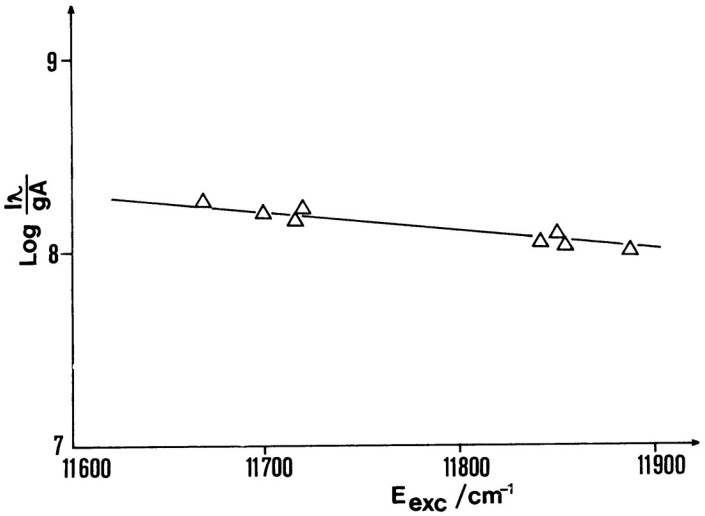

Figure 1. Boltzmann plot for AR I lines.

obtained by plotting $\log I\lambda/gA$ (for Ar lines — Figure 1) and $\log I\lambda^3/gf$ (for Fe lines — Figure 2) as a function of E_{exc}, where I is the spectral line intensity, λ is the wavelength, g is the statistical weight for each level, A is the transition probability, f is the atomic oscillator-strength and E_{exc} is the excitation energy of the employed argon and iron levels. The employed argon and iron lines with their excitation energy are listed in Table II. As argon levels listed in Table II are very near to each other and determination of the slope is not precise, the Fe lines are also used to confirm the value of the temperature.

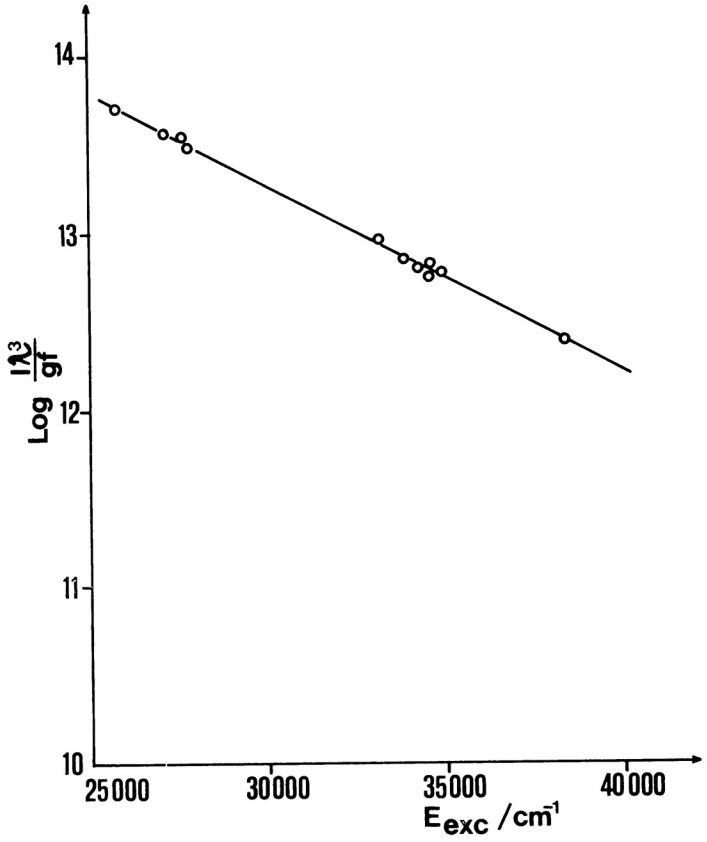

Figure 2. Boltzmann plot for Fe I lines.

According to study[12], the data for transition probabilities obtained by Malone and Carcoran[13] result in the best straight line, and these data were employed in our calculations. Using the data for the Fe atomic lines listed in Table II, and applying the slope method, the excitation temperature was calculated. Transition probabilites for the Fe lines were taken from[19]. Being of greater sensitivity, the absolute line intensity of Ar I 430.01 nm was used for determination of the excitation temperature. Using this method, temperature was measured according to the procedure described elsewhere[16]. As the absolute intensity of Ar I 430.01 nm line is used for temperature measurements, calibration of the spectrometer is required. Calibration was performed using tungsten filament as light source. Physical parameters and atomic constants for calculation of the emission coefficient of Ar line were taken from[17,18].

TABLE II

Argon and iron spectral lines used for temperature measurements

Ar *I* (nm)	E_{exc} (cm^{-1})	Fe *I* (nm)	Ex_{exc} (cm^{-1})
425.118	116660	370.925	34339
425.936	118870	373.332	27666
426.629	117183	376.379	34574
427.217	117115	373.487	33695
430.010	116999	375.824	34329
433.356	118469	373.713	27167
433.534	118459	374.826	27560
434.517	118407	374.949	34040
		381.584	38175
		382.043	33096
		382.444	26140

Measurement of Electron Number Density

The H_β (486.133 nm) line was chosen for the electron number density, n_e, measurements because it is a strong line, efficiently broadened for precise measurements but essentially not overlapping with its neighbours. It is located in a very accessible region in the spectrum and its selfabsorption is relatively small. The calculated electron density is accurate to about 7%, provided the other experimental errors can be kept small. Also, extensive Stark data are available for complete line profile[20].

The refined Stark theory, formulated by Griem, and the tabulated Stark parameter from Vidal *et al.*[21] were employed in our calculation. The 40-point profile of H_β was measured. Water was aspirated into the plasma for these measurements. A correction for instrumental and Doppler broadening was applied to the H_β profile before calculation of the electron number density. The instrumental profile was evaluated by using a low pressure mercury lamp and half width of the Hg I 435.8 nm, 410.8 nm and 491.6 nm lines were recorded. An instrumental width of about 0.06 nm was observed.

RESULTS AND DISCUSSION

Physical Parameters of the Discharge Excitation Temperature

The calculated temperatures, obtained by two different methods and by employing two different species (Fe and Ar lines), are listed in Table III.

Temperature measurements presented in Table III were taken at 15 mm above the load coil and at the carrier gas flow rate of 0.8 l/min. Experimental error in temperature determination was +/— 400 K. Differences between temperatures listed in Table III are within the limits of experimental error. Excitation temperatures were measured at different observation heights and for different carrier gas flow rates. The effect of carrier gas flow rate on

TABLE III

Calculated excitation temperatures

Method	Temperature (K)
absolute intensity of Ar *I* 430.01 nm line	6260
slope method (Ar *I* lines)	6170
slope methods (Fe *I* lines)	5940

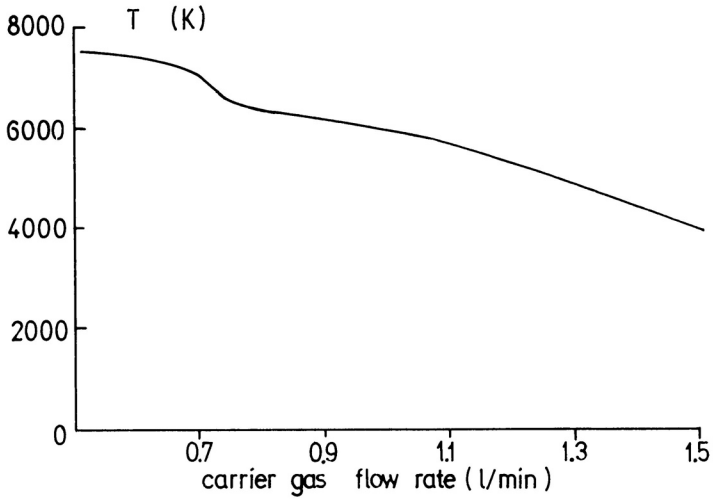

Figure 3. Excitation temperature as a function of the carrier gas flow rate at an observation height of 15 mm above the coil.

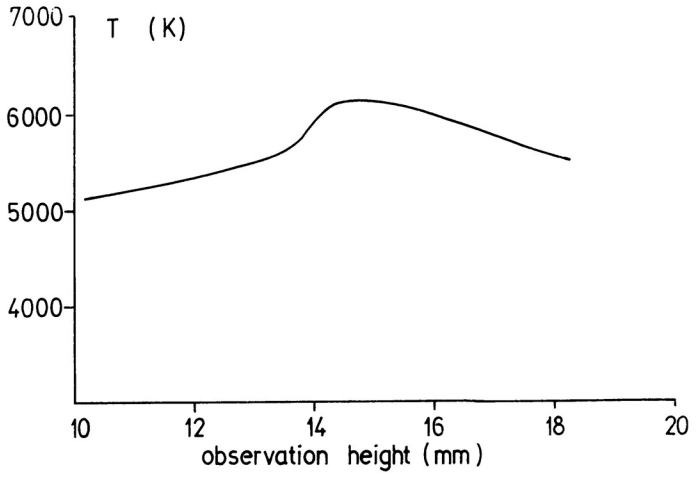

Figure 4. Excitation temperature as a function of the observation height at a carrier gas flow rate of 0.8 l/min.

the excitation temperature in the channel of an argon ICP is presented in Figure 3. The observation height was 15 mm above the load coil. Figure 3 shows that the temperature in the channel decreases by 3000 K. The decrease in temperature indicates that some changes might have occurred in the plasma characteristics. The influence of observation height on excitation temperature is presented in Figure 4. The maximum value of 6170 K was obtained at 15 mm above the load coil. The carrier gas flow rate during these measurements was 0.8 l/min. Since it was shown[12,15] that the differences between temperature measurements with and without Abel transformation are within the limits of experimental error, Abel transformation was not carried out.

Electron Number Density

The effect of carrier gas flow rate on the electron number density in the channel of an argon ICP is presented in Figure 5. The observation height was 15 mm above the load coil. The channel of an argon ICP could be expected to have very low values of the electron number density due to the cold gas stream. However, a moderately high electron number density was observed in the channel. This was attributed to ambipolar diffusion of electrons from the hot; high n_e annular region into the aerosol gas stream. As it can be seen from Figure 5, the electron number density in the channel decreases when the carrier gas flow rate increases. Figure 6 shows the plot of the electron number density as a function of observation height. The

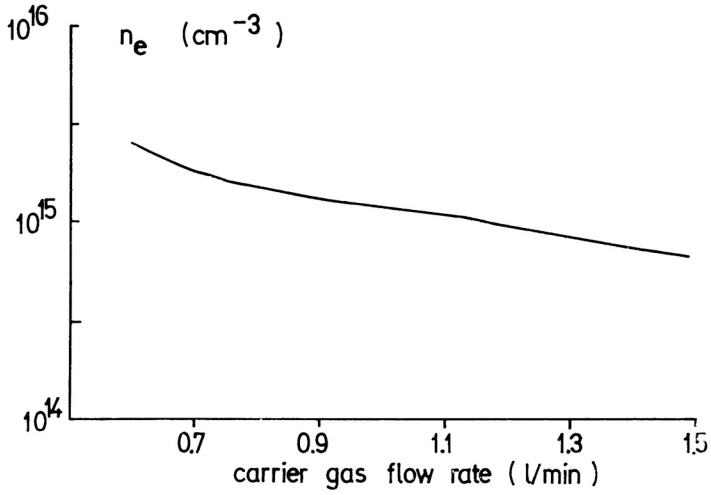

Figure 5. Electron number density as a function of gas flow rate.

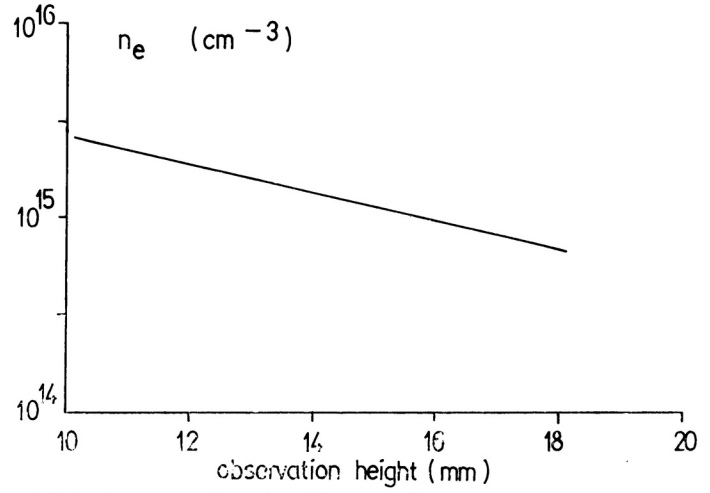

Figure 6. Electron number density as a function of observation height.

carrier gas flow rate was 0.8 l/min. The values of electron number density range from 4×10^{15} cm^{-3} to 7×10^{14} cm^{-3}. Figure 6 shows a fairly smooth drop in electron number density with observation height. Lack of Abel transformation should not affect the validity of the measured electron number density, especially for an observation height greater than 8 mm above the load coil[15].

Axial Distribution of Analytes in the Channel of an Argon ICP

Atom and ion lines with the excitation energy and ionization potential of the elements for which the axial distribution was studied are listed in Table IV.

TABLE IV

Atom (I) and ion (II) lines with excitation energies and ionization potentials of the considered elements

Spectral line (nm)			Excitation energy (eV)	Ionization energy (eV)
Cd	I	228.802	5.41	8.99
Cd	II	226.502	5.47	
Zn	I	213.856	5.80	9.39
Zn	II	202.548	6.01	
Mg	I	285.213	4.35	7.64
Mg	II	279.553	4.43	
Ca	I	422.673	2.94	6.11
Ca	II	393.366	3.15	
Cr	I	357.869	3.46	6.76
Cr	II	205.552	6.03	
Cu	I	324.754	3.82	7.72
Cu	II	224.700	8.23	
V	II	311.071	4.33	6.74
V	I	437.886	3.11	
Co	II	228.616	5.84	7.86
Mn	II	257.610	4.81	7.43
Mn	I	279.482	4.44	
Ni	I	232.003	5.34	7.63
Ni	II	221.644	6.63	
Sr	I	460.733	2.69	5.69
Sr	II	407.733	3.04	

In order to evaluate the influence of the changes in observation heights and carrier gas flow rates on analyte emission, the axial distribution of several ionic and atomic lines was measured. The ratios of net-line intensity I_n to background intensity I_b as a function of observation height for atomic and ionic lines of some elements are presented in Figure 7. Atom lines of Cu, Mn, Mg and Ca with excitation potential less than 5 eV (Table IV) have the maximum value at a lower observation height (12 mm) and atomic line of Cd and Zn with excitation potential 5.41 eV and 5.80 eV peak at a higher observation height (14 mm). Ionic lines of the studied elements peak between 14 and 16 mm above the load coil. 15 mm above the load coil under the

experimental condition cited above can be considered as a normal analytical zone (NAZ), which is in accordance with the visual blue ionic emission when a 1000 μg ml^{-1} Y solution was aspirated into the plasma.

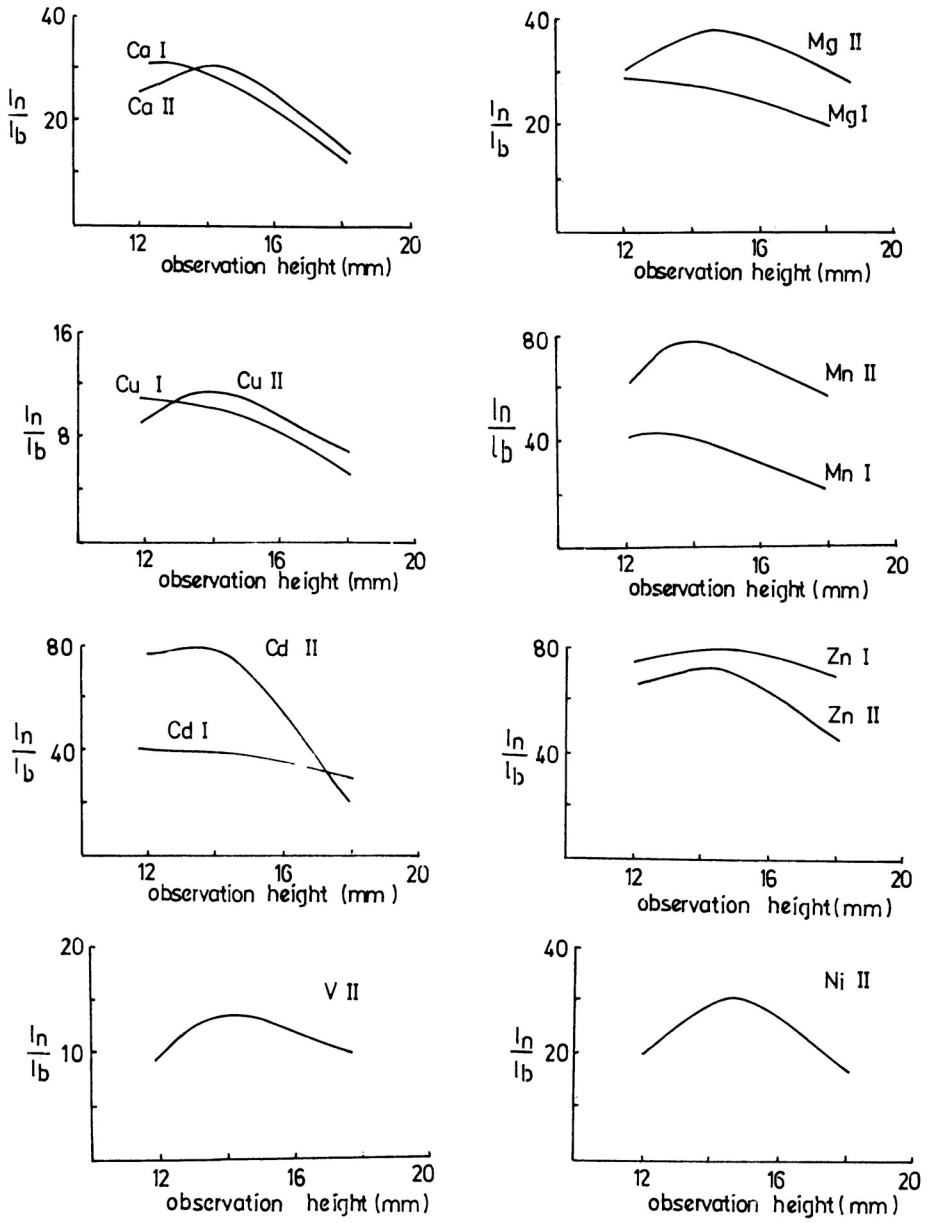

Figure 7. I_n/I_b as a function of observation height for atomic and ionic lines of some elements.

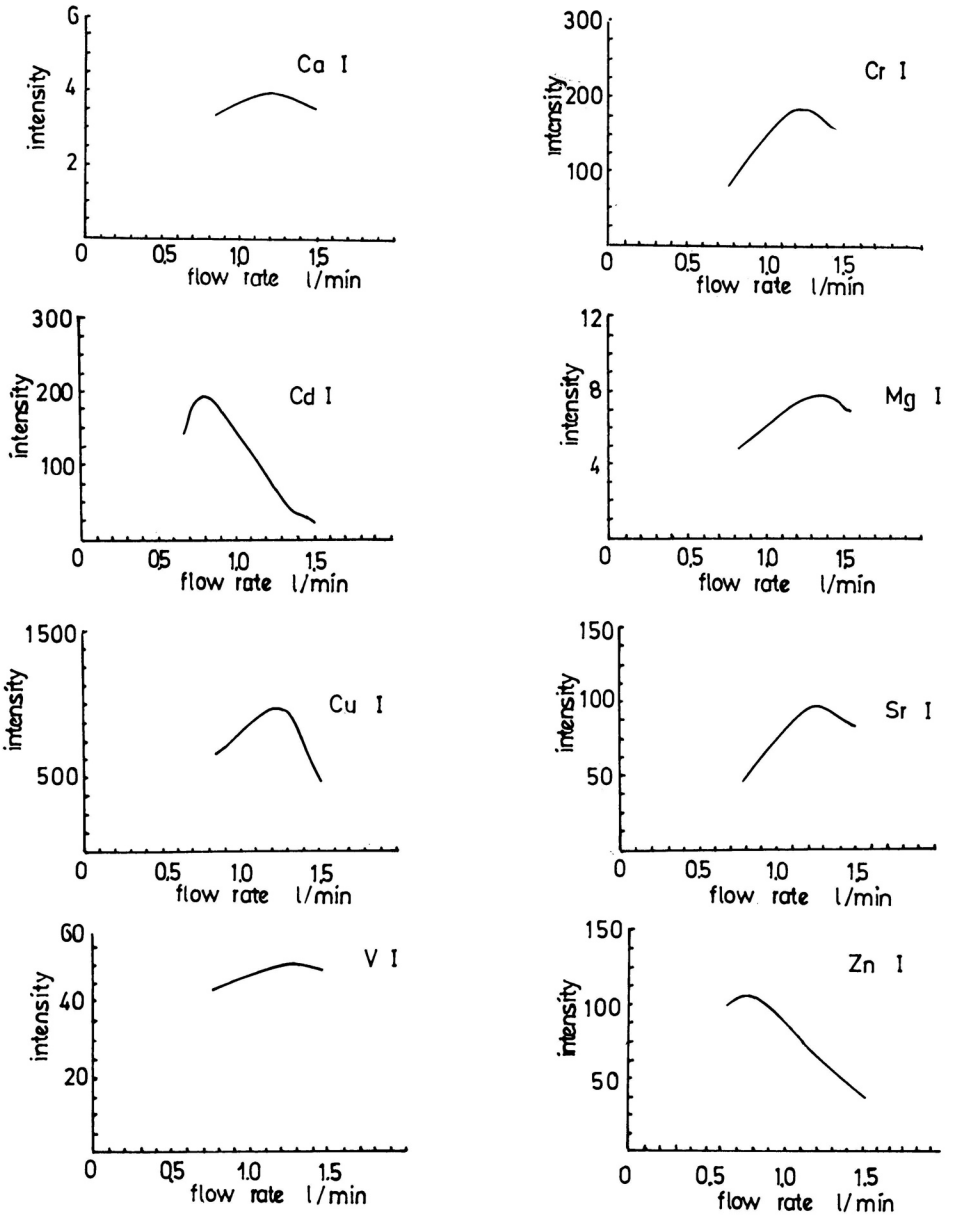

Figure 8. Net-line intensity (I_n) as a function of the carrier gas flow rate for atomic lines of some elements.

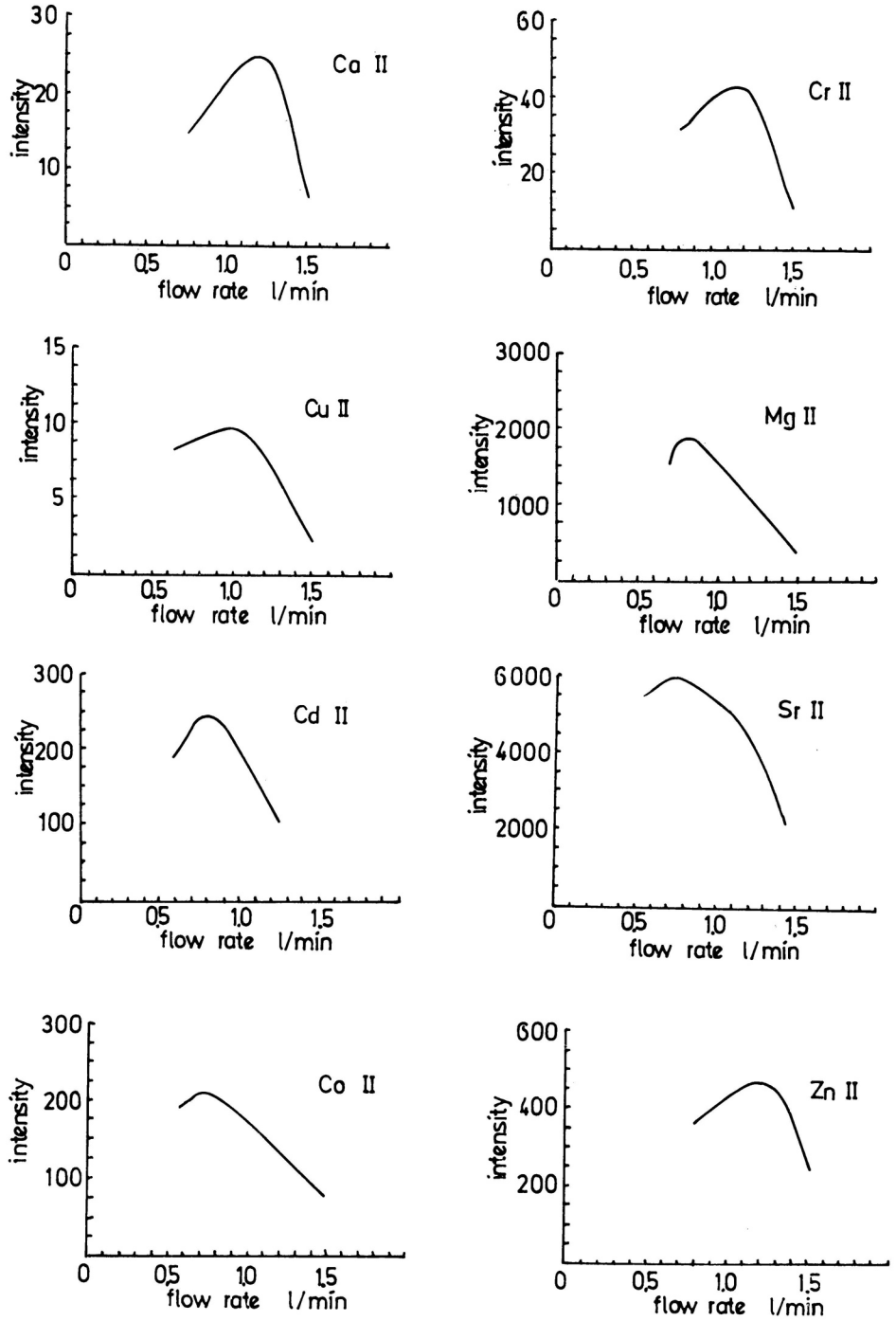

Figure 9. Net-line intensity (I_n) as a function of the carrier gas flow rate for ionic lines of some function.

The effects of the carrier gas flow rate on the net-line intensity emission of the atom and ion lines are presented in Figures 8 and 9. Atom lines of Ca, Cr, Cu, V and Sr have a maximum intensity at about 1.2 l/min. Ion lines of Mg, Co, Sr, Cd as well as Zn and Cd atom lines peak at a carrier gas flow rate of 0.8 l/min. Axial distribution of the studied analytes in this work is in agreement with the previously reported data.[1-11]

Approach to LTE

The channel of an argon ICP is a complex environment and is out of LTE. Recent publications[23-26] discussed the extent of departure from LTE. Introducing parameter b_r, it was possible to discuss the extent of departure from LTE. According to Caughlin and Blades[24], the b_r value can be defined as:

$$b_r = \frac{(I_i/I_a)_{exp}}{(I_i/I_a)_{LTE}}$$

where $(I_i/I_a)_{exp}$ represents the experimental measured ion-atom emission intensity ratio while $(I_i/I_a)_{LTE}$ stands for the ratio calculated under the LTE conditions, according to the theory outlined in[25]. The b_r value of 1 would correspond to a situation in which the experimentally measured ion-atom ratios are LTE values. Ion-atom emission intensity ratios have been measured for Ca, Sr, Zn and Cd. The ionization potential for these elements varies from 6—9 eV. For the calculation of $(I_i/I_a)_{LTE}$, the measured electron number density, n_e was used. These n_e values were used as input data for the LTE description of ICP and serve for comparison with experimental observation. All the necessary values of the constants for this calculation were taken from[22]. All the studied elements exhibit b_r values less than one.

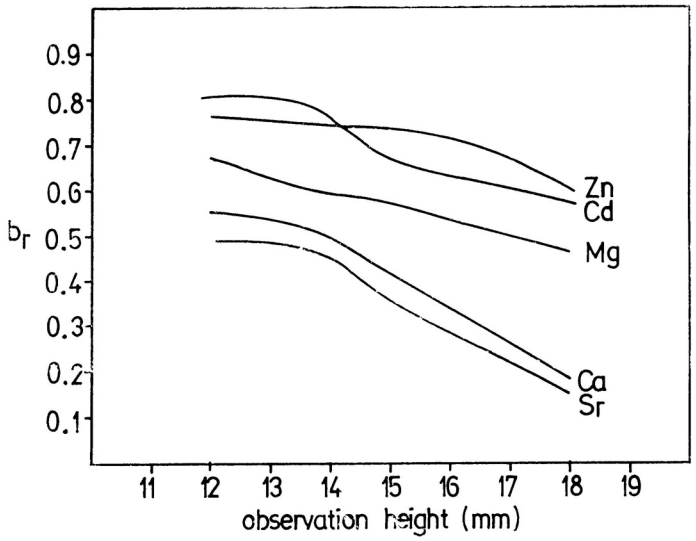

Figure 10. Experimental ion-atom intensity ratio to LTE ion-atom intensity ratio as a function of the observation height.

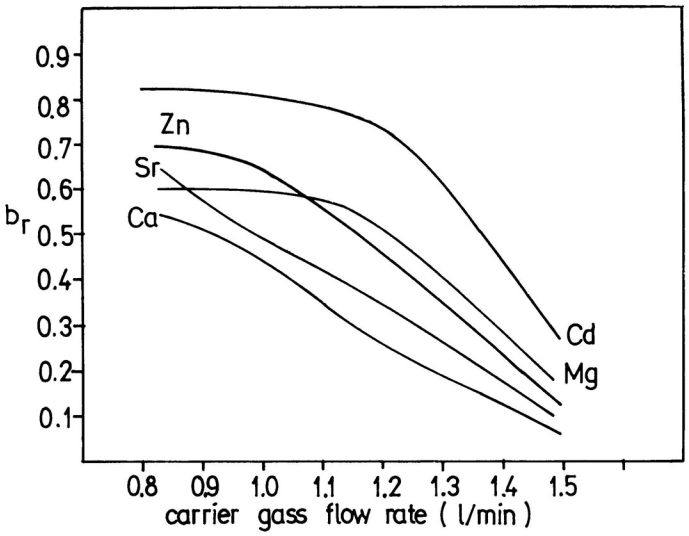

Figure 11. Experimental ion-atom intensity ratio to LTE ion-atom intensity as a function of the carrier gas flow rate.

Values less than one are characterized under ionization of analytes. With increasing observation height and carrier gas flow rate, the b_r values for Cd, Zn, Ca, Sr and Mg decrease, as shown in Figures 10 and 11. The b_r values for all studied elements at the power of 1.2 kW depend strongly on the observation height and the carrier gas flow rate. The highest b_r values are obtained for the carrier gas flow rate of 0.8 l/min and for the observation height of 15 mm above the load coil. The departure from LTE is increased when both the carrier gas flow rate and the observation height increase.

CONCLUSION

From the results presented above, it can be concluded that the changes in carrier gas flow rate and observation height significantly influence the measured analytical signal. A single observation height can be selected as almost optimal for ion lines. During a routine analytical procedure, these two parameters should be precisely defined and kept constant.

REFERENCES

1. P. W. J. M. Boumans and F. J. DeBoer, *Spectrochim. Acta* **30B** (1975) 309.
2. W. M. Blades and G. Horlick, *Spectrochim. Acta* **36B** (1981) 861.
3. W. M. Blades and G. Horlick, *Spectrochim. Acta* **36B** (1981) 881.
4. T. Edmonnds and G. Horlick, *Appl. Spectrosc.* **1** (1977) 536.
5. G. Dube and M. I. Bulous, *Can. J. Spectrosc.* **31** (1977) 536.
6. L. A. Fernando and N. Kovačić, *Fresenius Z. Anal. Chem.* **322** (1985) 547.
7. R. S. Houk and J. A. Olivares, *Spectrochim. Acta* **39B** (1984) 75.
8. P. W. J. M. Boumans, *ICP Newslett.* **4** (1978) 899.
9. P. W. J. M. Boumans and F. J. DeBoer, *Spectrochim. Acta* **27B** (1972) 391.
10. H. Kawaguchi, T. Ito, K. Ota, and A. Mizuike, *Spectrochim. Acta* **35B** (1980) 199.
11. H. Uchida, *Spectrosc. Letters* **14** (1981) 665.
12. J. Jarosz, J. M. Mermet, and J. P. Robin, *Spectrochim. Acta* **33B** (1978) 55.

13. B. S. Malone and W. H. Carcoran, *J. Quant. Spectrosc. Radiat. Transfer* **6** (1966) 443.
14. D. J. Kalnicky and V. A. Fassel, *Appl. Spectrosc.* **31** (1977) 2.
15. B. D. Webb and M. B. Dennton, *Spectrochim. Acta* **41B** (1988) 361.
16. N. Kovačić *Bull. Chem. Soc., Beograd* **48** (1983) 531.
17. P. Ranson and J. Chapelle, *J. Quant. Spectrosc. Radiant Transfer* **14** (1974) 1.
18. W. L. Wiese, M. W. Smith, and B. M. Miles, *Atomic Transition Probabilities, NSRDS-NBS 22,* Washington, D. C. (1968).
19. I. Reif, A. V. Fassel, R. N. Kniseley, and D. J. Kalnicky, *Spectrochim. Acta* **33B** (1978) 807.
20. H. R. Griem, *Spectral Line Broadening by Plasma,* Academic Press, New York, 1974.
21. C. R. Vidal, J. Copper, and E. W. Smith, *Astrophys. J. Suppl.* **25** (1973) 37.
22. W. L. Wiese and G. A. Martin, *Wavelengths and Ionization Probabilities for Atoms and Ions, Part II, NSRDS-NBS-68,* Washington, D. C. 1980.
23. I. J. M. M. Raaijmakers, P. W. J. M. Boumans, V. van der Sijde, and D. C. Schram, *Spectrochim. Acta* **38B** (1983) 697.
24. B. L. Caughlin and M. W. Blades, *Spectrochim. Acta* **40B** (1985) 1539.
25. B. L. Caughlin and M. W. Blades, *Spectrochim. Acta* **39B** (1984) 1583.
26. J. A. M. van der Mullen, I. J. M. W. Raaijmakers, A. C. A. P. van Lammern, D. C. Schram, B. van der Sijde, and H. J. W. Schenkelaars, *Spectrochim. Acta* **42B** (1987) 1039.

IZVLEČEK

Vpliv pretoka plina in višine opazovanja na intenziteto spektralnih črt v ICP izvoru

N. Kovačić, B. Budič, E. Kozak in V. Hudnik

Pretok nosilnega plina in višine opazovanja vplivata na elektronsko gostoto, temperaturo plazme in na intenziteto spektralnih črt v ICP izvoru. Prikazani so rezultati meritev aksialne porazdelitve intenzitete številnih atomskih in ionskih spektralnih črt v odvisnosti od obeh parametrov.